The Journal of Neuroscience, January 15, 2000, *20*(2):511–520

Ultrafast Inactivation Causes Inward Rectification in a Voltage-Gated K^+ Channel from *Caenorhabditis elegans*

Richard Fleischhauer,[1] M. Wayne Davis,[2] Igor Dzhura,[3] Alan Neely,[3] Leon Avery,[2] and Rolf H. Joho[1]

[1]*Center for Basic Neuroscience and* [2]*Department of Molecular Biology, The University of Texas Southwestern Medical Center at Dallas, Dallas, Texas 75390-9111, and* [3]*Department of Physiology, Texas Tech University Health Science Center, Lubbock, Texas 79430*

The *exp-2* gene in the nematode *Caenorhabditis elegans* influences the shape and duration of the action potential of pharyngeal muscle cells. Several loss-of-function mutations in *exp-2* lead to broadening of the action potential and to a concomitant slowing of the pumping action of the pharynx. In contrast, a gain-of-function mutation leads to narrow action potentials and shallow pumping. We cloned and functionally characterized the *exp-2* gene. The *exp-2* gene is homologous to genes of the family of voltage-gated K^+ channels (Kv type). The *Xenopus* oocyte-expressed EXP-2 channel, although structurally closely related to Kv-type channels, is functionally distinct and very similar to the human ether-à-gogo-related gene (HERG) K^+ channel. In response to depolarization, EXP-2 activates slowly and inactivates very rapidly. On repolarization, recovery from inactivation is also rapid and strongly voltage-dependent. These kinetic properties make the Kv-type EXP-2 channel an inward rectifier that resembles the structurally unrelated HERG channel. Apart from many similarities to HERG, however, the molecular mechanism of fast inactivation appears to be different. Moreover, the single-channel conductance is 5- to 10-fold larger than that of HERG and most Kv-type K^+ channels. It appears that the inward rectification mechanism by rapid inactivation has evolved independently in two distinct classes of structurally unrelated, voltage-gated K^+ channels.

Key words: potassium channel; Kv channel; inward rectifier; C. elegans*; pharyngeal muscle;* Xenopus *oocyte*

To maintain long-lasting action potentials (APs), voltage-gated K^+ channels are required that do not conduct at high levels during the plateau phase. Inward-rectifying K^+ channels have been shown to be important for the proper repolarization of APs with long plateaus (Hille, 1992). So far, two structurally different classes of inward rectifiers have been identified: tetrameric channels consisting of subunits with either two transmembrane (2-TM) or six transmembrane (6-TM) segments. The 2-TM-type channels may be activated by hyperpolarization without previous depolarization and derive the property of inward rectification from block of outward K^+ current by intracellular polyamines or Mg^{2+} ions (Dascal et al., 1993; Ho et al., 1993; Kubo et al., 1993). Two functionally different 6-TM-type inward rectifiers are known: the human ether-à-gogo-related gene (HERG) channel (Sanguinetti et al., 1995; Trudeau et al., 1995) and the plant inward rectifiers KAT1 and AKT1 (Anderson et al., 1992; Sentenac et al., 1992). HERG channels are activated by depolarization but inactivate rapidly, leading to relatively small outward currents (Trudeau et al., 1995; Schönherr and Heinemann, 1996; Smith et al., 1996; Spector et al., 1996; Wang et al., 1996). In contrast to HERG, KAT1 channels are activated by hyperpolarization but not depolarization. Unlike 2-TM-type inward rectifiers, KAT1 activation reflects a channel-intrinsic mechanism and not simply the relief of block from intracellular Mg^{2+} ions (Hoshi, 1995; Schroeder, 1995). 2-TM and 6-TM inward rectifiers show sequence similarities to voltage-gated (Kv) K^+ channels in the ion conduction pathway. Outside this pore region, there is very limited, if any, similarity between HERG and Kv-type channels, except for the fact that each K^+ channel subunit contains six transmembrane segments.

Here, we present evidence for a novel type of inward rectifier. The *exp-2* gene of the nematode *Caenorhabditis elegans* has been found to determine the shape and duration of the AP of pharyngeal muscle cells (Davis et al., 1995, 1999; Davis, 1999). Several loss-of-function mutations in *exp-2* lead to dramatic broadening of the muscle APs with a concomitant slowing of the pumping action of the pharynx. In contrast, a gain-of-function mutation leads to narrow APs with fast and shallow pumping. Based on the physiological role in rapid repolarization of the pharyngeal muscle, which was reminiscent of the function of HERG in the human heart, we surmised that EXP-2 might be closely related to HERG. When the *exp-2* gene was isolated, however, it became clear that it was homologous to genes from the Kv-type family of voltage-gated K^+ channels (Davis, 1999; Davis et al., 1999).

Below, we show that the *Xenopus* oocyte-expressed EXP-2 channel is functionally very similar to the HERG channel, although it is structurally closely related to Kv-type channels. EXP-2 activates slowly in response to depolarization and inactivates very rapidly. On repolarization, EXP-2 channels recover rapidly from inactivation in a strongly voltage-dependent manner. In contrast to HERG and most voltage-gated K^+ channels, EXP-2 has a relatively large unit conductance.

MATERIALS AND METHODS

Synthesis of EXP-2 cRNA

The identification and isolation of cDNA encoding EXP-2 is described in detail elsewhere (Davis, 1999). Briefly, a fully-spliced EXP-2 cDNA

Received Aug. 23, 1999; revised Oct. 20, 1999; accepted Oct. 21, 1999.

This work was supported in part by National Institutes of Health Grants NS28407 (R.H.J.), HL46154 (L.A.), and GM53196 (A.N.). We thank Dr. Gail Robertson (University of Wisconsin Medical School) for the HERG cDNA clone and Dr. Donald Hilgemann for insightful comments and critical reading of this manuscript.

Correspondence should be addressed to Dr. Rolf H. Joho, Center for Basic Neuroscience, The University of Texas Southwestern Medical Center, 5323 Harry Hines Boulevard, Dallas, TX 75390-9111. E-mail: joho@utsw.swmed.edu.

(1595 bp) was inserted into the pT7 expression vector (a derivative of pSP64; Cary et al., 1994) to allow *in vitro* transcription of cRNA that could be expressed in *Xenopus* oocytes. This vector contains a T7 promoter, 44 bases of the *Xenopus* β-globin 5′ untranslated region (UTR), and 143 bases of the *Xenopus* β-globin 3′ UTR followed by a poly(A) tract. The construct was linearized with *Bam*HI, and *in vitro* transcription was done using the Ribomax T7 kit (Promega, Madison, WI) to generate a cRNA 2134 nucleotides long. Capped transcripts were produced by the addition of 3 mM $m^7G(5')ppp(5')G$ (New England Biolabs, Beverly, MA) to the reaction.

Electrophysiology

Approximately 1–3 ng cRNA were injected into *Xenopus laevis* oocytes. After 1–4 d at 16°C, cells were subjected to a standard two-electrode voltage-clamp protocol (VanDongen et al., 1990) using an OC-725A amplifier (Warner Instruments, Hamden, CT). Experiments were done at room temperature (22 ± 1°C) in ND96 (96 mM NaCl, 2 mM KCl, 1 mM $MgCl_2$, and 1.8 mM $CaCl_2$ in 5 mM HEPES, pH 7.4) or in a solution in which KCl replaced NaCl. Both voltage-sensing and current-passing electrodes were filled with 3 M KCl and had resistances of 0.2–1.0 MΩ. The pCLAMP 6.0 software (Axon Instruments, Foster City, CA) was used to generate voltage pulse protocols and for data acquisition. Signals were filtered at 0.5–2.0 kHz and digitized at 1–10 kHz. Capacitive and leakage currents were not subtracted, and membrane potentials were not corrected for series resistance errors.

Macroscopic currents were also recorded using the cut-open oocyte voltage-clamp technique (Taglialatela et al., 1992) with a CA-1 amplifier (Dagan, Minneapolis, MN). The oocyte membrane exposed to the bottom chamber was permeabilized by a brief treatment with 0.1% saponin. The voltage electrodes contained 3 M KCl and had tip resistances from 0.6 to 1.2 MΩ. Data acquisition and analysis were performed using the pCLAMP system. External and internal solutions were the same as for the two-electrode voltage-clamp recording. Signals were filtered at 10 kHz and sampled at 20 kHz.

For single-channel recordings, experiments were essentially done as described previously (Moorman et al., 1990; Liu and Joho, 1998). Oocytes were kept in (in mM): 100 KCl, 1.0 $MgCl_2$, and 5.0 HEPES, pH 7.4. The pipette contained (in mM): 100 KCl, 1.0 $MgCl_2$, 1.8 $CaCl_2$, and 5.0 HEPES, pH 7.4, unless otherwise indicated. Analog signals were filtered at 2 kHz (Axopatch 200A and pCLAMP version 6.0), digitized at 86.6 kHz, and stored for off-line analysis. Passive leak and capacitance currents were subtracted using the mean of traces without channel openings. Single-channel data were analyzed using Fetchan and pSTAT (pCLAMP 6.0).

Data acquisition and analysis

The pCLAMP 6.0 software was used for data acquisition and to fit current traces to exponential functions.

Activation. Oocytes were depolarized for 1 sec to different potentials (from −80 to 60 mV), and the peaks of the inward tail currents (at −120 mV) were normalized to the maximal current. A conductance–voltage (*g–V*) relationship was fit to a Boltzmann equation, and the midpoint of activation ($V_{0.5}$) and the slope factor *k* were calculated.

To obtain the instantaneous *I–V* relationship, oocytes were depolarized to 20 mV for 1 sec to activate and inactivate EXP-2 channels. The channels were then allowed to recover for 20–40 msec at −80 or −120 mV before 200 msec test pulses in 10 mV increments were applied from −120 to 60 mV. For experiments with the cut-open oocyte, the instantaneous current amplitude was determined by extrapolating the tail current to the beginning of the test pulse. In cases of experiments with whole oocytes, the peak inward current was used, and the outward current was used after the capacitive component had settled (mean current from 5 to 10 msec after the onset of the test pulse). The latter approach underestimates the outward current at positive potentials and is probably the reason why almost no outward current is visible in Figure 3*C*.

The time dependence of activation was determined by varying the duration (1–4000 msec) of the depolarizing pulses at different voltages (−20 to 40 mV). The peaks of the tail currents (at −120 mV) were normalized to the maximum tail current, fit by a monoexponential function, and used to calculate the time constant for activation (τ_{act}).

Inactivation and deactivation. Deactivation and inactivation could be separated from each other because they differed greatly in their time and voltage dependence. After a 1 sec prepulse to 20 mV, channels were allowed to recover from inactivation for 20–40 msec at −80 or −120 mV. One second test pulses were applied in 10 mV increments to potentials in the range from −120 to 60 mV. To measure inactivation in the range from −60 to 0 mV (to +60 mV in the cut-open oocyte), the current representing the first 20 msec was fit with a monoexponential equation, which was then used to calculate the time constants of inactivation (τ_{inact}) at different voltages. In the voltage range in which the two-electrode voltage-clamp and cut-open oocyte techniques can be compared, the two approaches yielded similar results (see Fig. 5).

Deactivation could be separated from inactivation at test potentials more negative than −80 mV. The slow current decrease in the range from −80 to −120 mV was fit with a monoexponential function, which was used to calculate the time constants of deactivation (τ_{deact}).

Recovery from inactivation (deinactivation). Oocytes were depolarized for 1 sec to 20 mV to activate and inactivate EXP-2 channels. Channels were then allowed to recover from inactivation for 200 msec at different potentials from −60 to −120 mV. The rising phase of the tail current was well fit by a monoexponential function, which was used to calculate the time constants of recovery from inactivation (τ_{rec}) at different voltages.

Effects of external and internal tetraethylammonium. Inactivation and recovery from inactivation were studied in the presence of external or internal tetraethylammonium (TEA). A frog Ringer's solution containing 50 mM KCl and 50 mM TEA as monovalent ions was used to measure the effect of external TEA. To measure the effect of internally applied TEA, a 24 nl aliquot of a 1.0 M TEA solution was directly injected in the oocyte during the experiment. The volume of an oocyte was assumed to be 0.5×10^{-6} l (1 mm diameter).

RESULTS

The *C. elegans* gene *exp-2* is a member of the Kv family of voltage-gated K^+ channels

The *exp-2* gene of the nematode *C. elegans* is involved in the shape and duration of the pharyngeal muscle action potential (Davis, 1999). The action potential of wild-type pharyngeal muscle shows a characteristic plateau phase lasting 150–250 msec before rapid repolarization takes place, driving the membrane potential toward E_K. In loss-of-function mutations of *exp-2*, this plateau phase is dramatically prolonged and may last up to 6 sec (Davis et al., 1995; Davis, 1999). In contrast, an *exp-2* gain-of-function mutation (*sa26*) results in much briefer than normal action potentials (~50 msec). The action potential properties affected by these *exp-2* mutations led us to believe that the *exp-2* gene might encode a K^+ channel with properties similar to those of the HERG K^+ channel, which is involved in the rapid repolarization of the cardiac action potential. Indeed, the cloning of genomic DNA (and cDNA) encoding *exp-2* revealed an amino acid sequence of a putative K^+ channel (Davis, 1999; Davis et al., 1999). Contrary to expectation, EXP-2 showed no similarity to HERG except for its putative transmembrane topology. The EXP-2 sequence was, however, clearly related to the Kv family of voltage-gated K^+ channels represented by the subfamilies *Shaker*, *Shab*, *Shaw,* and *Shal* in *Drosophila* and Kv1–Kv9 in mammals (Fig. 1, Table 1).

The *exp-2* gene encodes a protein of 528 amino acid residues with a calculated molecular weight of 59,575 daltons. The EXP-2 protein has all the characteristics of Kv-type K^+ channels. It contains a hydrophobic core region with six putative transmembrane segments (S1–S6). The S4 segment contains six positively charged residues, and the linker region between S5 and S6 has the typical sequence of a potassium-selective ion channel (Hartmann et al., 1991; Yellen et al., 1991; Yool and Schwarz, 1991; Heginbotham et al., 1994). The hydrophobic core of EXP-2 is preceded by the conserved tetramerization domain T1, consisting of the subdomains A and B (Drewe et al., 1992; Li et al., 1992; Shen et al., 1993). The EXP-2 channel does not contain any consensus sites for cAMP-dependent protein kinase; it contains, however, three consensus sites for phosphorylation by protein kinase C (T131, T309, and S407). The extracellular S1–S2 linker region shows two consensus sites for N-glycosylation. Two such consen-

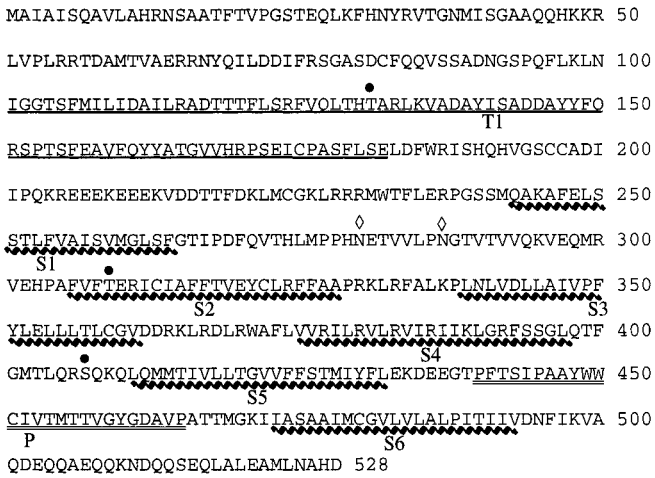

Figure 1. The EXP-2 channel is closely related to voltage-sensitive K^+ channels of the Kv type. The amino acid sequence of the *C. elegans* channel EXP-2 is shown in single-letter code. The tetramerization domain T1 is *underlined,* and the transmembrane segments S1–S6 are highlighted by a *wavy line*. The pore region between S5 and S6 is *doubly underlined*. Three consensus sites for phosphorylation by protein kinase C and two glycosylation sites are shown above the sequence by a *black dot* and a *diamond*, respectively. There are no consensus sites for phosphorylation by cAMP-dependent protein kinase. The amino acid sequence of EXP-2 is from Davis (1999).

sus sites at similar positions in *Shaker* are indeed glycosylated in insect cells and in oocytes (Santacruz-Toloza et al., 1994).

When the EXP-2 amino acid sequence was compared with the sequences of several other Kv-type channels, we found 35–43% identity, a value that is typical for K^+ channels that are members of different Kv subfamilies (Table 1). In contrast, K^+ channels from the same subfamily are 61–84% identical. EXP-2 had previously been placed in the *Shab* subfamily of K^+ channels (Wei et al., 1996); however, our analysis presented in Table 1 does not allow an assignment of EXP-2 to any of the known Kv subfamilies. It is possible that EXP-2 is not the *C. elegans* ortholog of a *Drosophila* or mammalian channel gene from one of the known Kv subfamilies but represents the prototype member of a novel subfamily of Kv channels (in this case Kv10).

The Kv-type channel EXP-2 acts as an inward rectifier

We injected *Xenopus* oocytes with cDNA-derived RNA (cRNA) to study the biophysical properties of EXP-2 channels. Oocytes were subjected to a two-electrode voltage-clamp protocol to determine voltage-dependent channel kinetics and ion selectivity. Initial experiments were done in frog Ringer's solution containing 100 mM KCl. To determine the voltage dependence of activation, oocytes were held at −80 mV, and depolarizing 1 sec test pulses were applied in 10 mV increments to 60 mV. The depolarizing test pulses were followed by 200 msec pulses to −120 mV (Fig. 2). During the 1 sec pulses, we could not detect any substantial steady-state outward current, even at potentials as positive as 60 mV; however, we consistently saw large inward-directed tail currents during the subsequent 200 msec pulses to −120 mV. These tail currents were visible only when the preceding 1 sec test pulses were to potentials more positive than −40 mV (Fig. 2*A*). Apparently, EXP-2 channels become activated during depolarization but inactivate rapidly, so little steady-state outward current can be observed during the 1 sec depolarization, a behavior reminiscent of HERG channels (Trudeau et al., 1995; Smith et al., 1996; Spector et al., 1996; Wang et al., 1996). On repolarization to −120 mV, again similar to HERG, EXP-2 channels recover rapidly from inactivation and generate large tail currents. We used the peak values of the tail currents to determine the *g–V* relationship of EXP-2 (Fig. 2*A, inset*). The midpoint of activation was $V_{0.5}$ = − 17 ± 2 mV (n = 5) with slope k = 6.5 ± 0.3 mV per e-fold change in conductance (n = 5).

To obtain the time constants for channel activation at different voltages, the duration of the depolarizing pulse was varied from 1 to 4000 msec in the range from −20 to 40 mV, and the fraction of activated channels was measured as the relative amplitude of the tail current evoked during the subsequent 200 msec pulse to −120 mV (Fig. 2*B*). Time constants were obtained from a single exponential function fit to the experimental data obtained at each voltage. Like the structurally unrelated HERG channel and unlike most other Kv-type channels, EXP-2 activates very slowly even at positive potentials. At 0 mV, the time constant for activation was 191 ± 23 msec (n = 5). Activation of EXP-2 showed a strong voltage dependence with time constants of 788 ± 117 msec at −20 mV (n = 5) to 35 ± 4 msec at 40 mV (n = 10) (see Fig. 5). Given the function of EXP-2 in repolarization after

Table 1. Amino acid sequence of EXP-2

	EXP-2	Sh	Kv1.1	Shab	Kv2.1	Shaw	Kv3.1	Shal	Kv4.1	Kv5.1	Kv6.1	Kv8.1	Kv9.1
EXP-2	100	35	35	41	43	35	34	37	38	41	35	40	38
Sh		100	**84**	43	46	48	46	44	45	39	36	40	37
Kv1.1			100	44	46	47	47	44	44	39	38	38	40
Shab				100	**76**	47	46	41	40	47	44	49	48
Kv2.1					100	49	48	42	41	48	48	52	48
Shaw						100	**61**	43	44	41	38	38	36
Kv3.1							100	44	44	42	40	39	39
Shal								100	**83**	37	37	40	35
Kv4.1									100	39	37	39	36
Kv5.1										100	39	42	41
Kv6.1											100	44	44
Kv8.1												100	49
Kv9.1													100

Amino acid sequences were compared across several segments that allowed direct alignment without gaps (A and B subdomains of T1, S1, S2–S3, S4–S5, and pore-S6; for details, see Drewe et al., 1992). The percent sequence identity is shown and highlighted in boldface for members of the same subfamily.

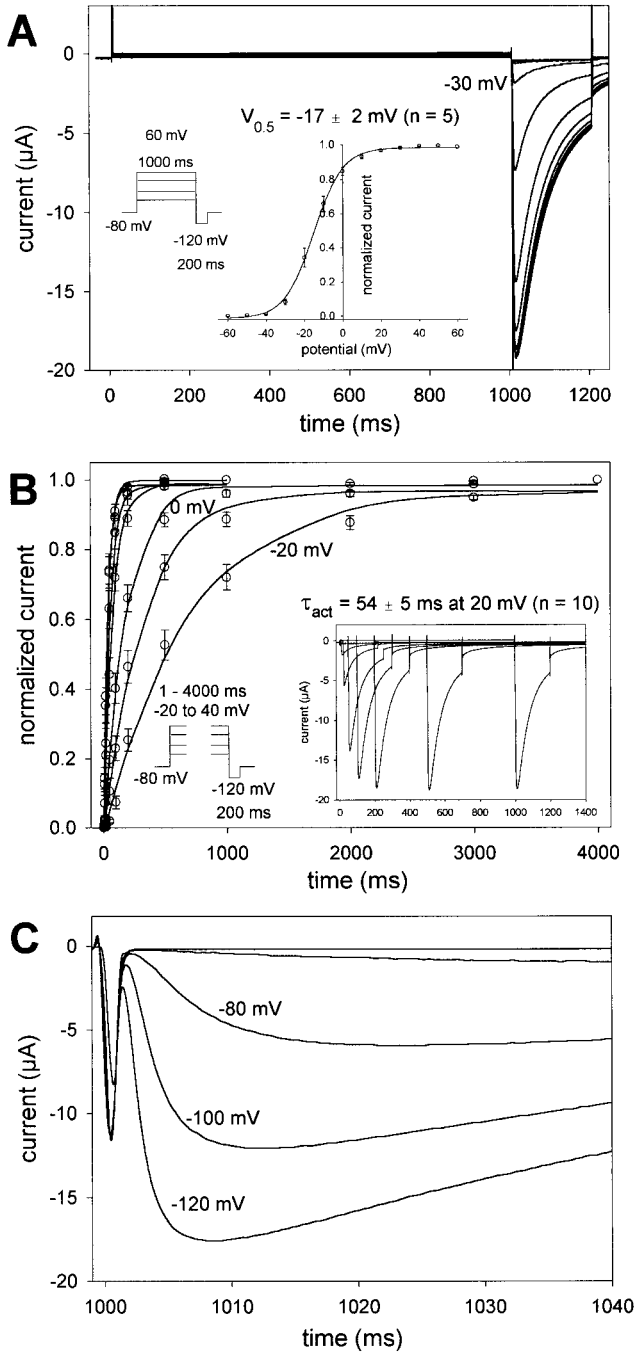

Figure 2. Voltage and time dependence of EXP-2 activation and recovery from inactivation. *A,* Oocytes were held at −80 mV, and 1 sec test pulses to potentials from −60 to 60 mV were applied in 10 mV increments, followed by 200 msec pulses to −120 mV. The first inward tail current could be detected at −30 mV, indicating the onset of activation of EXP-2 channels. *Inset, g–V* curve with a midpoint of activation $V_{0.5}$ = −17 ± 2 mV and slope k = 6.5 ± 0.3 mV per e-fold change in conductance (n = 5 oocytes). *B,* Oocytes were held at −80 mV, and test pulses to potentials from −20 to 40 mV were applied lasting from 1 to 4000 msec. The time dependence of EXP-2 activation was determined from the peak tail currents during the subsequent pulses to −120 mV. *Inset,* Actual recording at 20 mV. In *A* and *B*, oocytes were bathed in 100 mM KCl in frog Ringer's solution, and current traces were not leak-subtracted. *C,* EXP-2 channels were activated by 1 sec prepulses to 20 mV. Two hundred millisecond test pulses to different potentials from −120 to −60 mV were applied to initiate recovery from inactivation. Recovery from inactivation is faster at more negative potentials, indicating its steep voltage dependence.

long action potential plateaus (150–200 msec), relatively slow activation is consistent with its putative physiological role.

Because the voltage and time dependence of activation and the apparent fast inactivation of EXP-2 were reminiscent of the structurally unrelated HERG channel, we compared these two channels directly (Fig. 3). Oocyte-expressed EXP-2 or HERG channels were activated by 1 sec prepulses to 20 mV, followed by 40 msec pulses to −80 mV. Channels activated and inactivated during the 1 sec prepulses to 20 mV. During the 40 msec pulses to −80 mV, tail currents rise, indicating that EXP-2 channels have begun to recover from inactivation (τ_{rec} = ~4 msec) before they begin to deactivate slowly under these conditions (Fig. 3*A*). When the voltage is changed to −120 mV at the end of the 40 msec pulse, there is further time-dependent current increase before the onset of deactivation, which proceeds relatively slowly even at −120 mV. This additional current probably reflects channels that have not yet recovered from inactivation after 40 msec at −80 mV but recover under more hyperpolarized conditions. When the voltage was changed to less negative potentials, we could detect an initial rapid component of current decay (Fig. 3*A, arrow* at −60 mV). This decline in current was faster than deactivation, was strongly voltage dependent, and probably results from EXP-2 channels entering the inactivated state again. Hence, it appears that EXP-2 channels recover rapidly from inactivation at −80 mV but begin to inactivate again at less negative potentials, explaining the apparent lack of a steady-state outward current at positive test potentials. HERG channels also recover from inactivation at −80 mV, although more slowly than EXP-2 (Fig. 3*B*). Inactivation of HERG is, however, much slower than that of EXP-2, leading to detectable outward K^+ currents at potentials >0 mV (Fig. 3*B, arrow*), as has been shown previously (Schönherr and Heinemann, 1996; Smith et al., 1996; Spector et al., 1996; Wang et al., 1997). It seems that inactivation of EXP-2 is too fast for outward K^+ currents to be measured using the two-electrode voltage-clamp protocol in *Xenopus* oocytes. Uninjected control oocytes never showed any currents like the ones described for EXP-2 (Fig. 3*D*).

We determined the instantaneous *I–V* relationship and the selectivity for K^+ ions. At the end of the 40 msec recovery period (after the 1 sec depolarizing prepulse to 20 mV), test pulses to different potentials from −120 to 60 mV were applied to measure the instantaneous current through open EXP-2 channels before the onset of inactivation or deactivation. We used different extracellular K^+ concentrations to measure inward and, possibly, outward currents as a function of voltage and E_K (Fig. 3*C*). As expected for a K^+-selective channel, inward currents could only be seen in voltage ranges more negative than E_K. It was, however, difficult to determine the reversal potential for EXP-2 channels. Outward currents were very small even under conditions of relatively slow inactivation because of the concomitant small driving forces in the negative potential range (Fig. 3*C*). EXP-2 channels are more permeable for K^+ than Rb^+ ions. With 100 mM RbCl in the bath solution, tail currents were ~30% compared with currents in the presence of 100 mM KCl (data not shown).

Voltage dependence of inactivation and recovery from inactivation

The experiments described above suggested that EXP-2 may inactivate too rapidly for outward currents to be detected using

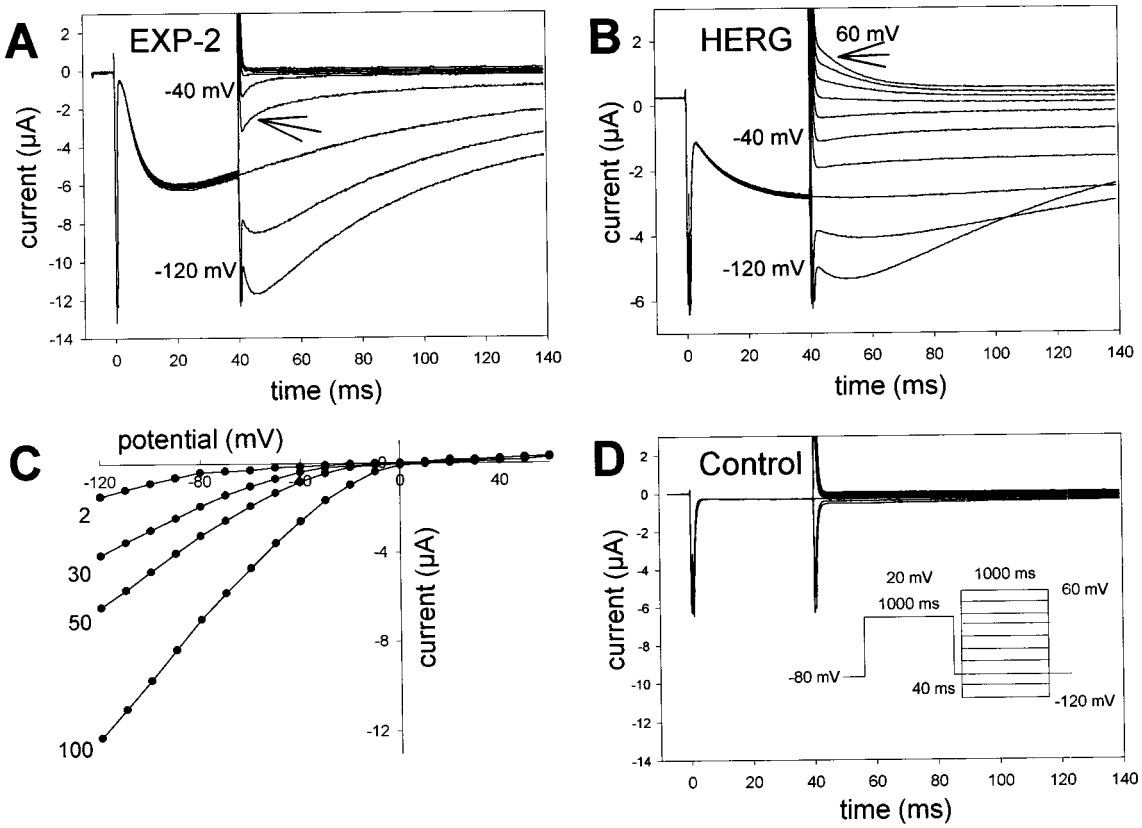

Figure 3. Instantaneous *I–V* relationship of EXP-2. *A,* EXP-2 channels were activated and inactivated by 1 sec prepulses to 20 mV and then allowed to recover from inactivation at −80 mV for 40 msec. After recovery from inactivation, the instantaneous current through open channels was determined for the beginning of 1 sec test pulses applied in 10 mV increments ranging from −120 to 60 mV. The *arrow* points to current decline attributable to rapid channel inactivation at −60 mV. No outward currents could be detected at positive potentials. *B,* HERG channels show little inactivation at negative potentials and outward current at positive potentials (*arrow* at 60 mV). *C, I–V* relationship for EXP-2 at different extracellular KCl concentrations, ranging from 2 to 100 mM (same oocyte). Inward currents are only detectable at voltages more negative than E_K, indicating the potassium selectivity of EXP-2. *D,* Uninjected control oocytes show no EXP-2-like currents. The same pulse protocol was used for experiments presented in *A*, *B*, and *D*.

the two-electrode voltage clamp on whole oocytes. We therefore used the cut-open oocyte technique, which provides much faster voltage control and time resolution (Taglialatela et al., 1992). Using a similar pulse protocol as above, we could clearly detect outward K^+ currents, both in 2.5 and 100 mM extracellular K^+ ions (Fig. 4). With 100 mM KCl in the bath, the currents reversed direction at approximately −5 mV, close to the expected value of E_K. In 2.5 mM extracellular KCl, outward K^+ currents could be detected at potentials positive to approximately −60 mV, again indicating that EXP-2 channels are selective for K^+ over Na^+ ions. An increase in the extracellular potassium concentration increases EXP-2 channel conductance despite a decrease in driving force, a phenomenon observed for several voltage-gated K^+ channels and inward rectifiers (Hille, 1992; Pardo et al., 1992; López-Barneo et al., 1993).

We also determined the voltage dependence of deactivation, inactivation, and recovery from inactivation. To study the voltage dependence of inactivation and deactivation, EXP-2 channels were activated and inactivated by a 1 sec prepulse to 20 mV, followed by a 20 msec pulse to −120 mV during which all channels recovered from inactivation (Fig. 4). At this point, 1 sec test pulses were applied in 10 mV increments between −120 and 60 mV. To determine the time constant of inactivation, the first 20 msec of the current traces in the voltage range from −60 to 0 mV were fitted with a single exponential. This initial process is mainly governed by inactivation that becomes faster at less negative potentials (see Figs. 3*A*, 4*B, arrows*). Deactivation time constants were determined in the potential range from −80 to −120 mV in which inactivation is relatively slow and can be neglected. To determine the time and voltage dependence of recovery from inactivation, EXP-2 channels were activated by 1 sec prepulses to 20 mV, followed by 200 msec test pulses to different potentials from −60 to −120 mV (Fig. 2*C*). The rising phase of the currents was fit to a monoexponential function and used to determine time constants for the recovery from inactivation at different voltages.

The time constants for activation (τ_{act}), deactivation (τ_{deact}), inactivation (τ_{inact}), and recovery from inactivation (τ_{rec}) were used to calculate the corresponding apparent transition rates as a function of voltage (Fig. 5). As expected, the rates for activation are strongly voltage-dependent and nearly semilogarithmic from −20 to 20 mV. In contrast, deactivation rates show no voltage dependence and are relatively small (~13/sec) between −120 and −80 mV. Both the rates for inactivation and recovery from inactivation are strongly voltage-dependent and up to ~100 times greater than the rates for activation or deactivation at similar voltages. Hence, it appears that inactivation and recovery from inactivation are strongly voltage-dependent like the corresponding processes in HERG, although EXP-2 forms a Kv-type K^+ channel unrelated in sequence to HERG.

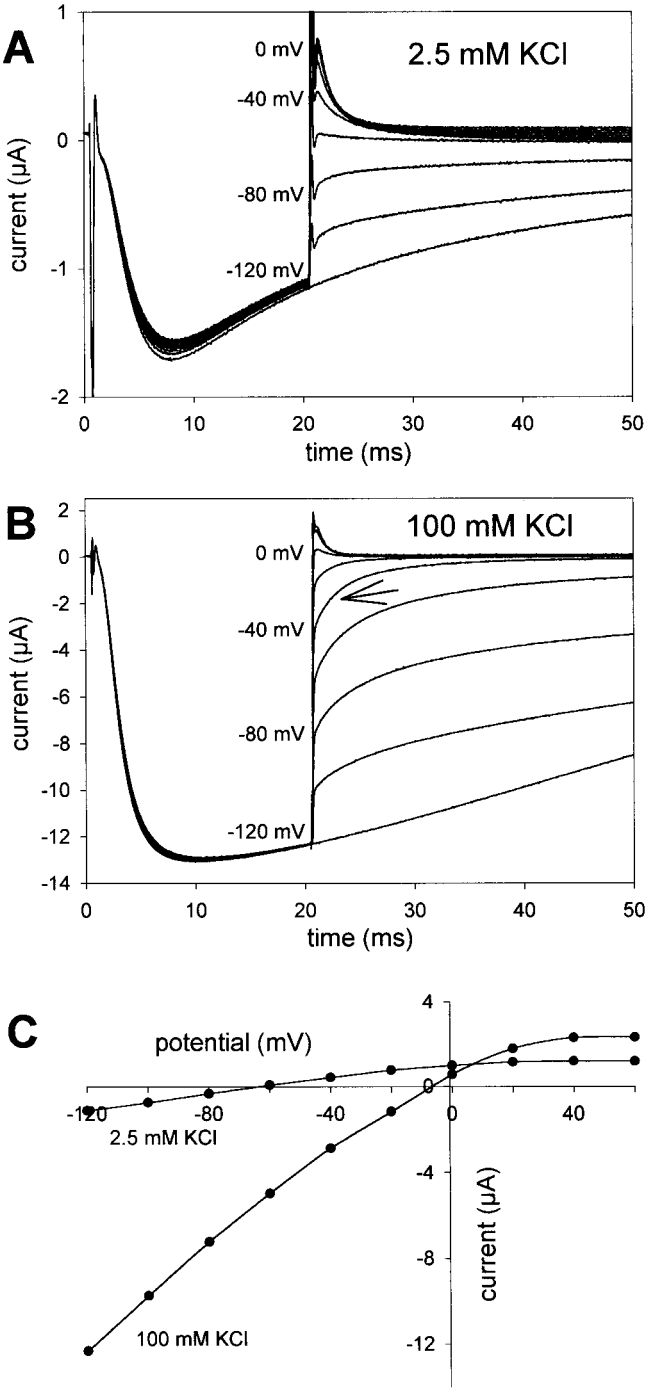

Figure 4. Inward rectification is caused by ultrafast inactivation. The cut-open oocyte technique was used to study fast inactivation. EXP-2 channels were activated and inactivated by 1 sec prepulses to 20 mV from a holding potential at −80 mV and then allowed to recover from inactivation for 20 msec at −120 mV. To determine the instantaneous current, the voltage was then stepped in 20 mV increments to different potentials from −120 to 60 mV. The *arrow* points to current decline attributable to rapid channel inactivation. *A,* With 2.5 mM KCl in the bath, the current reversed direction at approximately −60 mV. *B,* In 100 mM KCl, outward and inward currents are larger, and the current reversed direction at ~0 mV. *C, I–V* relationship in 2.5 and 100 mM extracellular KCl solution (same oocyte).

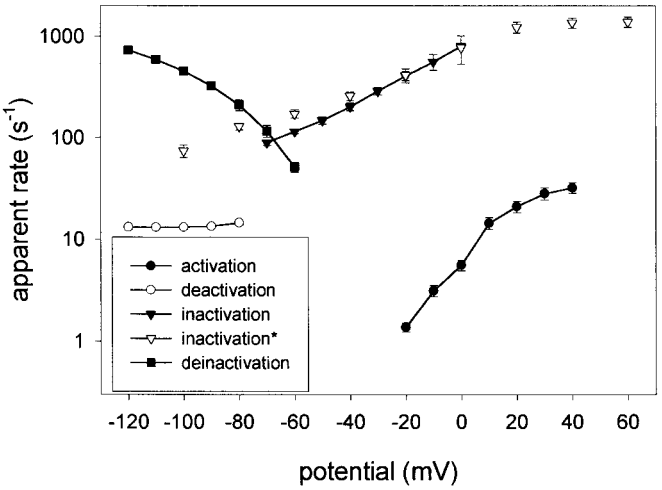

Figure 5. Apparent transition rate constants of EXP-2. The apparent voltage-dependent rate constants (per second) for activation, inactivation, recovery from inactivation (deinactivation), and deactivation were calculated as the reciprocal values of the corresponding time constants τ_{act}, τ_{inact}, τ_{rec}, and τ_{deact}. It is apparent that inactivation and recovery from inactivation is up to ~100 times faster than activation. Deactivation is very slow and not voltage-dependent between −80 and −120 mV. *Open inverted triangles* (inactivation) indicate data points obtained with the cut-open oocyte technique; all other data were obtained using the two-electrode voltage clamp on whole oocytes.

Internal TEA blocks EXP-2 channels and slows fast inactivation

Kv-type K^+ channels have been shown to undergo two distinct types of inactivation (Choi et al., 1991; Hoshi et al., 1991). The relatively fast N-type inactivation involves the binding of an N-terminal particle of a single-channel subunit to the cytoplasmic face or inner vestibule of the channel, thereby occluding the pore and preventing ion flow (Hoshi et al., 1990). The inactivation particle corresponds to a segment of ~20 amino acids at the N terminus of each channel subunit. In contrast; the relatively slow C-type inactivation involves some conformational changes near the outer end of the ion conduction pathway (Hoshi et al., 1991; Yellen et al., 1994). TEA, a common blocker of K^+ channels that can act on the extracellular or intracellular side, is often used to differentiate between these two types of inactivation. Blockade by extracellular TEA leads to a slowing of C-type inactivation, presumably by interfering with conformational rearrangements in the outer mouth of the pore, without affecting N-type inactivation (Yellen et al., 1994). Intracellular TEA competes with the N-terminal blocking particle slowing N-type inactivation, but it has no effect on C-type inactivation (Choi et al., 1991). To determine whether the ultrafast inactivation process of EXP-2 might be of N or C type, we investigated the effect of external and internal TEA on the current amplitude and inactivation kinetics. Extracellular TEA blocked EXP-2 channels in a concentration-dependent manner with an IC_{50} (at −70 mV) of 30 ± 13 mM (n = 3) without affecting the kinetics of inactivation (Fig. 6*A*). To study the action of TEA from the inside, we injected TEA in EXP-2-expressing oocytes to an intracellular concentration of ~50 mM. At this concentration, the inward potassium current (at −70 mV) was reduced to 51 ± 6% of control (n = 3). In contrast to extracellular TEA, which did not affect inactivation, intracellular TEA slowed inactivation approximately twofold (Fig. 6*B*). It appears therefore that the ultrafast inactivation process in EXP-2

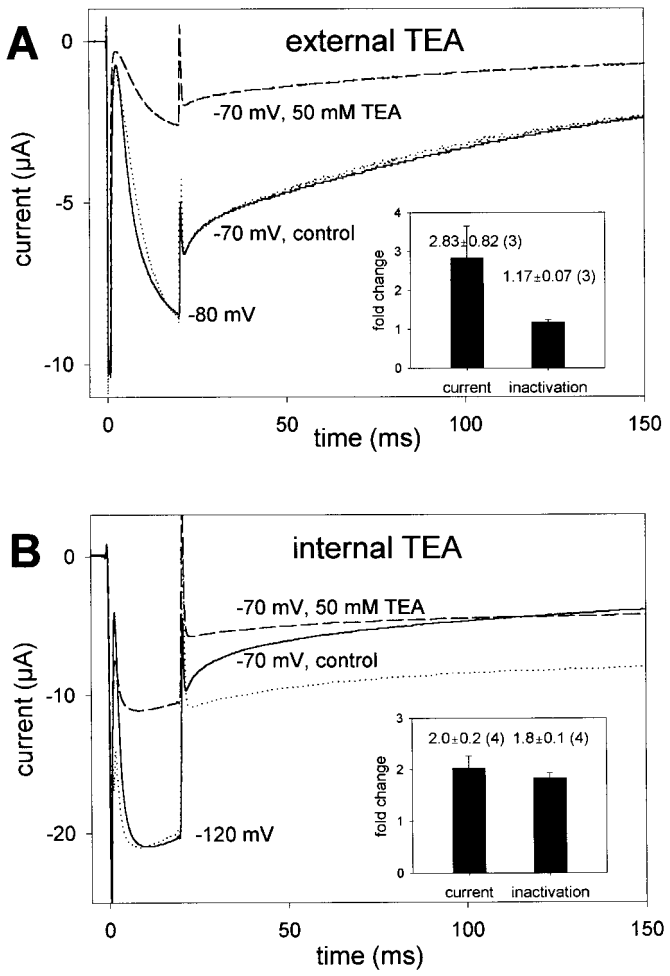

Figure 6. Effect of external and internal TEA on inactivation. Fully activated and inactivated EXP-2 channels were allowed to recover from inactivation for 20 msec at −80 or −120 mV, followed by a test pulse to −70 mV to determine the time course of inactivation. *A,* External application of 50 mM TEA reduces the current amplitude after recovery from inactivation to 31% of control without changing the kinetics of current decay. The *dotted line* represents the current trace in the presence of TEA scaled to match the control current at the end of recovery from inactivation. *Inset,* Nearly threefold reduction of current (to 41 ± 10% of control, mean ± SEM; $n = 3$) without changing the inactivation time constant. *B,* Internal application of ~50 mM TEA reduces the current to 53% of control and slows inactivation. The *dotted line* represents the scaled current trace in presence of TEA for direct comparison with the control trace. *Inset,* Twofold current reduction and a twofold increase in the inactivation time constant (mean ± SEM; $n = 4$).

is similarly slowed by internal TEA like N-type inactivation in *Shaker*.

EXP-2 is a large conductance channel

We used cell-attached patches of EXP-expressing oocytes to measure the conductance of single EXP-2 channels. From a holding potential at −80 mV, EXP-2 channels were activated (and inactivated) by 1 sec prepulses to 20 mV, followed by test pulses ranging from −60 to −150 mV during which EXP-2 channels recover from inactivation (Fig. 7*A*). With 100 mM KCl in the recording pipette, EXP-2 channels showed unitary currents that increased with more negative test potentials. During subsequent steps to 40 mV, we were unable to detect outward current through single channels, presumably because inactivation proceeds too rapidly ($\tau_{inact} = 0.7$ msec at 40 mV). The *I–V* relationship was linear from −150 to 0 mV with a chord conductance of 67 ± 2 pS and an extrapolated reversal potential of −0.35 mV ($n = 5$). The ensemble average for recovery from inactivation derived from 200 single-channel traces was similar to that of traces obtained from macroscopic recordings using the two-electrode voltage clamp (Fig. 7*B*).

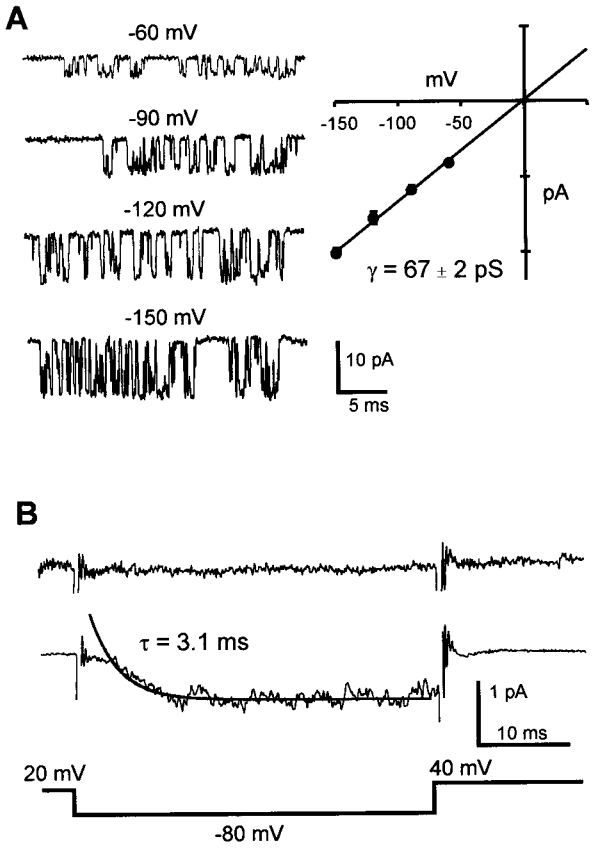

Figure 7. Single-channel currents from EXP-2 channels. Single-channel activity was recorded during recovery from inactivation with 100 mM KCl in the recording pipette. Channel activation and inactivation were induced by a 1 sec prepulse to 20 mV. *A,* The voltage for recovery was varied from −60 to −150 mV. Representative *traces* at all test voltages are shown in the *left panel*. The *right panel* shows the *I–V* relationship for single EXP-2 channels (5 different patches). Regression analysis yields a single-channel conductance of 67 ± 2 pS. *B,* Ensemble average currents for EXP-2 channels. *Top trace* (no prepulse) shows the average of 20 traces when the activation–inactivation prepulse to 20 mV was reduced to 4 msec. The *middle trace* shows the average of 200 traces and the superimposed single-exponential fit with a time constant of 3.1 msec. The *bottom trace* depicts the voltage protocol during sampling. Capacitive and leakage components were obtained from a multiexponential fit to the average of 10 traces with no openings. The idealized trace was then subtracted from each individual trace before averaging. The remaining frequency transients were blanked.

DISCUSSION

EXP-2 is a novel K^+ channel of the Kv family

We describe the functional characterization of the novel, voltage-gated K^+ channel EXP-2 which is expressed in pharyngeal muscle cells of the nematode *C. elegans* (Davis, 1999; Davis et al., 1999). Loss-of-function mutations in the *exp-2* gene cause dramatic prolongations of the muscle action potential; in contrast, a gain-of-function mutation leads to brief action potentials, indi-

Table 2. Kinetic parameters of EXP-2, voltage-gated K^+ channels (Kv), and HERG

	Kv Channels	EXP-2	HERG
Activation (msec)	Generally fast	Intermediate	Slow
τ at 20 mV	msec range	54 ± 2	~100–300
Inactivation (msec)	Voltage independent, fast and slow	Voltage dependent, ultrafast	Voltage dependent, fast
τ at 20 mV	10s of msec (N type) to sec (C type)	0.8 ± 0.1, type unknown	~5–30, C type
Deinactivation (msec)	Variable	Fast	Fast
τ at −80 mV	~10–1000	5.6 ± 0.7	~8
Deactivation (msec)	Fast	Slow	Very slow
τ at −80 mV	~1–10, voltage dependent	70 ± 3, little voltage-dependent	~300–1000, Voltage dependent
TEA slows inactivation	From inside and outside	From inside	From outside
Unit conductance (pS)	Small to intermediate	Large	Small
In 100 mM KCl	~5–25	67 ± 2	12

The data for Kv channels are from Stühmer et al. (1989), Pak et al. (1991a,b), and Grissmer et al. (1994); the data for HERG are from Nakajima et al. (1998), Schönherr et al. (1996), Smith et al. (1996), Spector et al. (1996), Wang et al. (1996 and 1997), and Zou et al. (1997).

cating that *exp-2* may encode a voltage-controlled K^+ channel involved in rapid repolarization after the long plateau phase of the action potential (Davis, 1999; Davis et al., 1999). When we had cloned *exp-2* DNA, it became apparent that the encoded EXP-2 protein (528 amino acids) was very similar to voltage-gated K^+ channels of the Kv family (35–43% sequence identity to different Kv subfamilies) (Table 1). Although the *exp-2* gene had previously been placed in the *Shab* subfamily (Wei et al., 1996), our analysis shows only a marginally higher percentage of sequence identity to *Shab* or Kv2.1 (41 and 43%, respectively) compared with members of other Kv subfamilies (35–40%). In contrast, different members of the same subfamily are ~61–84% identical (Table 1). It is possible, therefore, that EXP-2 represents the prototype of a novel K^+ channel subfamily (to be designated Kv10) that has been found neither in *Drosophila* nor in vertebrates. The degree of sequence identity that delineates subfamilies is somewhat arbitrary. It has been shown that mainly channel subunits from the same subfamily form heterotetrameric K^+ channels (Christie et al., 1990; Isacoff et al., 1990; Ruppersberg et al., 1990; Covarrubias et al., 1991). More recently, it has become clear that members of the subfamilies Kv5, Kv6, Kv8, and Kv9, which do not form functional homotetramers, apparently associate with and modify the function of subunits from the subfamilies Kv2 and Kv3 (Hugnot et al., 1996; Salinas et al., 1997). It will be interesting to see whether EXP-2 subunits are able to co-assemble with subunits from other Kv subfamilies.

The EXP-2 channel contains three consensus sites for phosphorylation by protein kinase C (T131, T309, and S407) and two consensus sites for glycosylation in the extracellular linker region connecting S1 and S2. It is currently not known whether the activity of EXP-2 is modulated by phosphorylation or whether EXP-2 channels are glycosylated. It has been shown that two glycosylation sites at similar positions in the Shaker K^+ channel are indeed glycosylated (Santacruz-Toloza et al., 1994).

EXP-2 is a Kv-type channel acting as an inward rectifier

The kinetic behavior of EXP-2 is highly unusual for a channel that clearly belongs in the Kv family of voltage-gated K^+ channels (Table 2). Kv-type channels show relatively fast voltage-dependent activation (with the exception of *Shaw*), slow C-type inactivation, and voltage-dependent deactivation. In addition, some Kv channels, e.g., *Shaker*, Kv1.4, and Kv3.4, also show fast N-type inactivation. Activation of EXP-2 channels is voltage-dependent but occurs relatively slowly even at positive potentials (τ_{act} = ~54 msec at 20 mV; Fig. 2). Deactivation is even slower and shows little or no voltage dependence between −80 and −120 mV (τ_{deact} = ~80 msec). The greatest differences from Kv-type K^+ channels can be seen for inactivation and recovery from inactivation. Both processes are voltage-dependent and occur at very fast rates compared with most Kv channels (Fig. 5). Inactivation begins to take place in the negative voltage range (τ_{inact} = ~8 msec at −60 mV) and occurs very rapidly at positive voltages (τ_{inact} = ~0.8 msec at 20 mV). Recovery from inactivation also occurs very rapidly (τ_{rec} = ~5 msec at −80 mV and ~1 msec at −120 mV).

The putative physiological function of EXP-2 in pharyngeal muscle cells and the kinetics of oocyte-expressed channels are very reminiscent of the role and kinetic properties of the human cardiac K^+ channel HERG (Trudeau et al., 1995; Smith et al., 1996; Spector et al., 1996; Wang et al., 1996). Like HERG, EXP-2 shows voltage-dependent slow activation, fast inactivation, and fast recovery from inactivation. Interestingly, although EXP-2 and HERG show very similar kinetics of activation and inactivation, the two channels are not homologous and show no sequence similarity outside the pore region. It is remarkable that the inward rectification mechanism by rapid inactivation has evolved independently in two classes of structurally unrelated voltage-gated K^+ channels.

To our knowledge, EXP-2 is the only Kv-type K^+ channel that is known to function as an inward rectifier in a normal physiological environment. The outwardly rectifying *Shaker* channel was converted to an inward rectifier by S4 mutations leading to channel activation at approximately −200 mV (Miller and Aldrich, 1996). In contrast to EXP-2, which is activated at approximately −20 mV and derives its inward rectification from the ultrafast inactivation mechanism, the *Shaker* S4 mutants are already activated and have undergone steady-state inactivation at the resting membrane potential. EXP-2 channels require depolarization before they can open; in contrast, the *Shaker* S4 mutants can be activated by hyperpolarization.

Internal TEA blocks EXP-2 and slows inactivation

TEA blockade can be used to distinguish N-type from C-type inactivation in voltage-gated K^+ channels (Choi et al., 1991). Although TEA blocks EXP-2 from either side, only blockade from the inside slows inactivation (Fig. 6). The twofold change, both in current reduction and in the slowing of inactivation, is

expected if internal TEA occluded ion flux by competing with the N-terminal inactivation particle for binding to the inner vestibule. The TEA effect on inactivation is clearly different between EXP-2 and HERG, although the two channels behave similarly in many other aspects (Table 2). In contrast to EXP-2, external TEA slows inactivation of HERG, and this has been interpreted as a form of fast C-type inactivation in HERG (Schönherr et al., 1996; Smith et al., 1996). The finding that external TEA blocks EXP-2 without slowing inactivation does not rule out the presence of C-type inactivation, which might be slow and masked by faster N-type-like inactivation. Also, it has been shown that some quaternary ammonium ions block from the inside and affect conformational changes of the outer mouth that are involved in C-type inactivation (Baukrowitz and Yellen, 1996). Future experiments involving the removal of the N terminus will be needed to determine whether a *Shaker*-type "ball-and-chain" mechanism underlies the voltage-dependent, ultrafast inactivation in EXP-2.

Besides the apparent difference in the underlying molecular mechanism of fast inactivation, another difference from HERG (and other Kv channels) is the large unit conductance of EXP-2. Single EXP-2 channels show a unit conductance of 67 ± 2 pS. This is 5–10 times larger than the conductances of many Kv channels (5–10 pS) with the exception of Kv3.1 (~25 pS). It is also substantially larger then the 12 pS conductance of HERG (Zou et al., 1997). We currently do not know the sequence differences in EXP-2 that cause the relatively large conductance.

Are the properties of EXP-2 suitable for the rapid repolarization after long-duration action potentials?

Intracellular recordings of pharyngeal muscle cells show action potentials with long plateaus (150–200 msec) followed by a rapid phase of repolarization. Several loss-of-function mutations in *exp-2* lead to dramatically prolonged action potentials, and a gain-of-function mutation results in brief action potentials (Davis et al., 1995). These findings suggest strongly that EXP-2 channels are directly involved in rapid repolarization, a role similar to HERG channels in the human heart. The question remains, however, whether homotetrameric EXP-2 channels are really suited for fast repolarization after a long plateau. Although EXP-2 channels activate slowly (τ_{act} = ~54 msec at 20 mV), >90% of channels become activated and inactivated (τ_{inact} = ~1 msec at 20 mV) during the ~150 msec plateau of the pharyngeal action potential. Hence, when the membrane potential approaches ~0 mV toward the end of the plateau phase, EXP-2 channels are "primed" for the rapid recovery from inactivation. The rate of recovery from inactivation is, however, still much slower than the inactivation rate (Fig. 5). This scenario is reminiscent of voltage-sensitive Na^+ channels in the situation when the membrane potential approaches the threshold for action potential generation. Under these threshold conditions, the rate of Na^+ channel activation is far slower than the inactivation rate; however, local depolarization followed by transient Na^+ channel openings eventually lead to regenerative channel openings resulting in the upstroke of the action potential. A current with the properties of EXP-2 was originally described in *Ascaris* by Byerly and Masuda (1979). These authors coined the term *negative spike channel* because of its similar but opposite action to voltage-sensitive Na^+ channels.

Of course, we cannot rule out that the function of EXP-2 channels in the pharyngeal muscle cells might be modified by other subunits. It is currently not known whether EXP-2 subunits in *C. elegans* pharyngeal muscle form homotetrameric channels, as assumed to be the case in *Xenopus* oocytes, or whether they co-assemble with other subunits in a heterotetrameric K^+ channel complex that is responsible for the fast repolarization of pharyngeal muscle cells.

REFERENCES

Anderson JA, Huprikar SS, Kochian LV, Lucas WJ, Gaber RF (1992) Functional expression of a probable *Arabidopsis thaliana* potassium channel in *Saccharomyces cerevisiae*. Proc Natl Acad Sci USA 89:3736–3740.

Baukrowitz T, Yellen G (1996) Use-dependent blockers and exit rate of the last ion from the multi-ion pore of a K^+ channel. Science 271:653–656.

Byerly L, Masuda MO (1979) Voltage-clamp analysis of the potassium current that produces a negative-going action potential in *Ascaris* muscle. J Physiol (Lond) 288:263–284.

Cary RB, Klymkowsky MW, Evans RM, Domingo A, Dent JA, Backhus LE (1994) Vimentin's tail interacts with actin-containing structures in vivo. J Cell Sci 107:1609–1622.

Choi KL, Aldrich RW, Yellen G (1991) Tetraethylammonium blockade distinguishes two inactivation mechanisms in voltage-activated K^+ channels. Proc Natl Acad Sci USA 88:5092–5095.

Christie MJ, North RA, Osborne PB, Douglass J, Adelman JP (1990) Heteropolymeric potassium channels expressed in *Xenopus* oocytes from cloned subunits. Neuron 4:405–411.

Covarrubias M, Wei A, Salkoff L (1991) Shaker, *Shal*, *Shab*, and *Shaw* express independent K^+ current system. Neuron 7:763–773.

Dascal N, Schreibmayer W, Lim NF, Wang W, Chavkin C, DiMagno L, Labarca C, Kieffer BL, Gaveriaux-Ruff C, Trollinger D, Lester HA, Davidson N (1993) Atrial G protein-activated K^+ channel: expression cloning and molecular properties. Proc Natl Acad Sci USA 90:10235–10239.

Davis MW (1999) Regulation of the relaxation phase of the *C. elegans* pharyngeal muscle action potential. PhD dissertation, The University of Texas Southwestern Medical Center at Dallas.

Davis MW, Somerville D, Lee RYN, Lockery S, Avery L, Fambrough DM (1995) Mutations in the *Caenorhabditis elegans* Na,K-ATPase α-subunit gene, *eat-6*, disrupt excitable cell function. J Neurosci 15:8408–8418.

Davis MW, Fleischhauer R, Dent J, Joho RH, Avery L (1999) EXP-2 is a K^+ channel involved in repolarization of pharyngeal muscle in *C. elegans.* Soc Neurosci Abstr 25:532.

Drewe JA, Verma S, Frech GC, Joho RH (1992) Distinct spatial and temporal expression patterns of K^+ channel mRNAs from different subfamilies. J Neurosci 12:538–548.

Grissmer S, Nguyen AN, Aiyar J, Hanson DC, Mather RJ, Gutman GA, Karmilowicz MJ, Auperin DD, Chandy KG (1994) Pharmacological characterization of five cloned voltage-gated K^+ channels, types Kv1.1, 1.2, 1.3, 1.5, and 3.1, stably expressed in mammalian cell lines. Mol Pharmacol 45:1227–1234.

Hartmann HA, Kirsch GE, Drewe JA, Taglialatela M, Joho RH, Brown AM (1991) Exchange of conduction pathways between two related potassium channels. Science 251:942–944.

Heginbotham L, Lu Z, Abramson T, MacKinnon R (1994) Mutation in the K^+ channel signature sequence. Biophys J 66:1061–1067.

Hille B (1992) Ionic channels of excitable membranes, Ed 2. Sunderland, MA: Sinauer.

Ho K, Nichols CG, Lederer WJ, Lytton J, Vassilev PM, Kanazirska MV, Hebert SC (1993) Cloning and expression of an inwardly rectifying ATP-regulated potassium channel. Nature 362:31–38.

Hoshi T (1995) Regulation of voltage dependence of the KAT1 channel by intracellular factors. J Gen Physiol 105:309–328.

Hoshi T, Zagotta WN, Aldrich RW (1990) Biophysical and molecular mechanisms of *Shaker* potassium channel inactivation. Science 250:533–538.

Hoshi T, Zagotta WN, Aldrich RW (1991) Two types of inactivation in *Shaker* K^+ channels: effects of alterations in the carboxy-terminal region. Neuron 7:547–556.

Hugnot JP, Salinas M, Lesage F, Guillemare E, Weille J, Heurtaux C, Mattθi MG, Lasdunski M (1996) Kv8.1, a new neuronal potassium channel subunit with specific inhibitory properties towards *Shab* and *Shaw* channels. EMBO J. 15:3322–3331.

Isacoff EY, Jan YN, Jan LY (1990) Evidence for the formation of het-

eromultimeric potassium channels in *Xenopus* oocytes. Nature 345:530–534.

Kubo Y, Baldwin TJ, Jan YN, Jan LY (1993) Primary structure and functional expression of a mouse inward rectifier potassium channel. Nature 362:127–132.

Li M, Jan YN, Jan LY (1992) Specification of subunit assembly by the hydrophilic amino-terminal domain of the Shaker potassium channel. Science 257:1225–1230.

Liu Y, Joho RH (1998) A side chain in S6 influences both open-state stability and ion permeation in a voltage-gated K^+ channel. Pflügers Arch 435:654–661.

L≤pez-Barneo J, Hoshi T, Heinemann SH, Aldrich RW (1993) Effects of external cations and mutations in the pore region on C-type inactivation of Shaker potassium channels. Receptors Channels 1:61–71.

Miller AG, Aldrich RW (1996) Conversion of a delayed rectifier K^+ channel to a voltage-gated inward rectifier K^+ channel by three amino acid substitutions. Neuron 16:853–858.

Moorman JR, Kirsch GE, VanDongen AMJ, Joho RH, Brown AM (1990) Fast and slow gating of sodium channels encoded by a single mRNA. Neuron 4:243–252.

Nakajima T, Furukawa T, Tanaka T, Katayama Y, Nagai R, Nakamura Y, Hiraoka M (1998) Novel mechanism of HERG current suppression in LQT2. Circ Res 83:415–422.

Pak MD, Covarrubias M, Ratcliffe A, Salkoff L (1991a) A mouse brain homolog of the *Drosophila Shab* K^+ channel with conserved delayed-rectifier properties. J Neurosci 11:869–880.

Pak MD, Baker K, Covarrubias M, Butler A, Ratcliffe A, Salkoff L (1991b) mShal, a subfamily of A-type K^+ channel cloned from mammalian brain. Proc Natl Acad Sci USA 88:4386–4390.

Pardo LA, Heinemann SH, Terlau H, Ludewig U, Lorra C, Pongs O, Stühmer W (1992) Extracellular K^+ specifically modulates a rat brain K^+ channel. Proc Natl Acad Sci USA 89:2466–2470.

Ruppersberg JP, Schröter KH, Sakmann B, Stocker M, Sewing S, Pongs O (1990) Heteromultimeric channels formed by rat brain potassium-channel proteins. Nature 345:535–537.

Salinas M, Duprat F, Heurtaux C, Hugnot JP, Lazdunski, M (1997) New modulatory α subunits for mammalian *Shab* K^+ channels. J Biol Chem 272:24371–24379.

Sanguinetti MC, Jiang C, Curran ME, Keating MT (1995) A mechanistic link between an inherited and an acquired cardiac arrhythmia: HERG encodes the I_{Kr} potassium channel. Cell 81:299–307.

Santacruz-Toloza L, Huang Y, John SA, Papazian DM (1994) Glycosylation of Shaker potassium channel protein in insect cell culture and in *Xenopus* oocytes. Biochemistry 33:5607–5613.

Schönherr R, Heinemann SH (1996) Molecular determinants for activation and inactivation of HERG, a human inward rectifier potassium channel. J Physiol (Lond) 493:635–642.

Schroeder JI (1995) Magnesium-independent activation of inward-rectifying K^+ channels in *Vicia faba* guard cells. FEBS Lett 363:157–160.

Sentenac H, Bonneaud N, Minet M, Lacroute F, Salmon JM, Gaymard F, Grignon C (1992) Cloning and expression in yeast of a plant potassium ion transport system. Science 256:663–665.

Shen NV, Chen X, Boyer MM, Pfaffinger PJ (1993) Deletion analysis of K^+ channel assembly. Neuron 11:67–76.

Smith PL, Baukrowitz T, Yellen G (1996) The inward rectification mechanism of the HERG cardiac potassium channel. Nature 379:833–836.

Spector PS, Curran ME, Zou A, Keating MT, Sanguinetti MC (1996) Fast inactivation causes rectification of the I_{Kr} channel. J Gen Physiol 107:611–619.

Stühmer W, Ruppersberg JP, Schröter KH, Sakmann B, Stocker M, Giese KP, Perschke A, Baumann A, Pongs O (1989) Molecular basis of functional diversity of voltage-gated potassium channels in mammalian brain. EMBO J 8:3235–3244.

Taglialatela M, Toro L, Stefani E (1992) Novel voltage clamp to record small, fast currents from ion channels expressed in *Xenopus* oocytes. Biophys J 61:78–82.

Trudeau MC, Warmke JW, Ganetzky B, Robertson GA (1995) HERG, a human inward rectifier in the voltage-gated potassium channel family. Science 269:92–95.

VanDongen AMJ, Frech GC, Drewe JA, Joho RH, Brown AM (1990) Alteration and restoration of K^+ channel function by deletions at the N- and C-termini. Neuron 5:433–443.

Wang S, Morales MJ, Liu S, Strauss HC, Rasmusson RL (1996) Time, voltage and ionic concentration dependence of rectification of h-*erg* expressed in *Xenopus* oocytes. FEBS Lett 389:167–173.

Wang S, Liu S, Morales MJ, Strauss HC, Rasmusson RL (1997) A quantitative analysis of the activation and inactivation kinetics of *HERG* expressed in *Xenopus* oocytes. J Physiol (Lond) 502:45–60.

Wei A, Jegla T, Salkoff L (1996) Eight potassium channel families revealed by the *C. elegans* genome project. Neuropharmacology 35:805–829.

Yellen G, Jurman ME, Abramson T, MacKinnon R (1991) Mutations affecting internal TEA blockade identify the probable pore-forming region of a K^+ channel. Science 251:939–942.

Yellen G, Sodickson D, Chen TY, Jurman ME (1994) An engineered cysteine in the external mouth of a K^+ channel allows inactivation to be modulated by metal binding. Biophys J 66:1068–1075.

Yool AJ, Schwarz TL (1991) Alteration of ionic selectivity of a K^+ channel by mutation of the H5 region. Nature 349:700–704.

Zou A, Curran ME, Keating MT, Sanguinetti MC (1997) Single HERG delayed rectifier K^+ channels in *Xenopus* oocytes. Am J Physiol 272: H1309–H1314.